

## ADDENDUM - EXXON FISCHER-TROPSCH WORK

### Fischer Synthesis Process

A patent (A.1), a continuation of four prior applications with the first dated October 3, 1989, claimed a method for hydrocarbon synthesis reactions. This patent relates to the use of a catalyst of the "rim" type, as the terminology is used by Exxon. These are catalysts where the active metal(s) are deposited in the outermost layer of the support particle, and in a manner that the interior of the support particle is essentially devoid of the metal(s). This approach is widely used in the manufacturer of auto exhaust catalysts that are shaped into spheres, cylinders, etc. The specific experiments were conducted with a 6 wt.% cobalt and 0.5 wt.% ruthenium on silica or titania support; since the surface area of the catalyst used in the example was reported to be about 20 m<sup>2</sup>/g it is assumed that the support was titania. The description of the preferred embodiment includes a derivation of the theoretical aspects of the determination of the rim loaded thickness needed to optimize CO conversion and/or minimize methane production. This theory has been included in several of the reviews of Fischer-Tropsch synthesis that have recently been published by Exxon workers. It is surprising that the authors of these reviews are not inventors of this method for hydrocarbon synthesis reactions and that the inventor (M. Herskowitz) is not an author of the review articles.

The outer layer containing the catalytic metal has a thickness determined so as to optimize CO conversion to heavy hydrocarbons so that conversion to methane is maintained at a predetermined level. The inventor maintains that it is not possible to simultaneously maximize CO conversion and minimize methane conversion. However it is possible to define a rim thickness so as to optimize one of these products. The

thickness of the rim-loaded catalyst is determined by relating the rate of diffusion of CO and H<sub>2</sub> to a rate of reaction in the porous inorganic oxide for a predetermined support geometry, partial pressures and temperatures.

The fluxes of the two reactants at steady state must be equal since there is no accumulation; thus,

$$\beta D_{e,CO} [dC_{CO}/d\tau] = D_{e,H} [dC_H/d\tau] \quad [A.1]$$

where the flux is expressed as a product of the effective diffusivity,  $D_e$ , and the concentration gradient.  $\beta$  is the stoichiometric coefficient and is equal to 2.07 in the reported work. Since hydrogen diffuses more rapidly than CO, the relative concentration of hydrogen should increase from the surface to the center of the catalyst pellet.

The differential mass balance inside the pores of the catalyst pellet of carbon monoxide, the limiting reactant, is

$$[D_{e,CO} (1/\tau^s)] d/d\tau[\tau^s (dC_{CO}/d\tau)] = \rho_p r_{CO} \quad [A.2]$$

where  $\tau$  is the radial position measured from the external surface toward the center,  $\rho_p$  is the pellet density,  $C_{CO}$  is the CO concentration in the liquid-filled pores and  $r_{CO}$  is the intrinsic rate of reaction on the active sites. The shape factor,  $s$ , is equal to two for a sphere and to unity for a cylinder; the treatment can be extended to other pellet shapes.

The boundary condition on the external surface is:

$$C_{CO} = P_{CO,b}/H_{CO} \quad [A.3]$$

where  $P_{CO,b}$  is the CO partial pressure in the bulk gas phase and  $H_{CO}$  is the Henry's Law constant. The other boundary condition can be defined for two cases as:

$$\text{inert core} \quad dC_{CO}/d\tau = 0 \quad \tau = \tau_i \quad [A.4]$$

$$\text{hollow core } C_{CO} - P_{CO,b}/H_{CO} = ? \quad [A.5]$$

This derivation assumes that external mass transfer resistance is negligible and that the pellet is isothermal. Experimental data verified that these are valid assumptions.

The intrinsic rate expression (small particle, diffusion free case) for cobalt or ruthenium on titania or silica support is

$$r_{CO} = k_1 \exp(-E_1/RT) [P_{CO}^a P_H^b / (1 + k_2 P_{CO} + k_3 P_H)^c] \quad [A.6]$$

where  $k_1$ ,  $k_2$ ,  $k_3$ ,  $E_1$ ,  $a$ ,  $b$ , and  $c$  are calculated from experimental rate data. [In this and other Exxon patents there are many typos that are usually obvious but sometimes cause concern. Thus, in the above equation we have modified the equation given in the patent by replacing 1 in the original with  $a$  and 2 with  $c$  to produce equation [A.6].]

The inventor indicates that the kinetic parameter,  $k_1$ , usually depends only on the metal concentration on the support; presumably the dispersion must also be included. The inventor indicates that in certain cases such as cobalt on titania, it is also a function of water partial pressure:

$$k_1 = A [(1 + k_4 P_{H_2O}) / (1 + (k_5 P_{H_2O})^2)] \quad [A.7]$$

where  $A$  is the activity of the catalyst.

Henry's Law can be used to express equation [A6] in concentrations of CO and  $H_2$ :

$$C_{CO} = P_{CO}/H_{CO} ; C_H = P_H/H_H \quad [A.8]$$

Integrating equation [A1] allows the expression of the hydrogen concentration in terms of the carbon monoxide concentration:

$$C_H = [P_{H,b}/H_H] - [\beta D_{e,CO}/D_{e,H}] [(P_{CO,b}/H_{CO}) - C_{CO}] \quad [A.9]$$

or

$$H_H C_H / P_{H,b} = 1 - \beta [1 - (H_{CO} C_{CO} / P_{CO,b})] \quad [A.10]$$

where

$$\beta = (\beta D_{e,CO}/D_{e,H})(H_H/H_{CO})(P_{CO,b}/P_{H,b}) \quad [A.11]$$

Substituting equations [A6] and [A7] into equation [A8] and expressing in dimensional-less form yields

$$f = (\beta_s - \beta_c) [\beta k_1 \exp(-E_1/RT) [P_{CO}^a P_H^b / D_{e,CO} (k_2 P_{CO,b})^c] ]^{1.2} \quad [A.12]$$

The Thiele modulus,  $f$ , is the ratio between the maximum rate of reaction and the maximum rate of diffusion. Likewise,  $\beta$  expresses the ratio between the maximum rate of diffusion of the two reactants; when  $\beta = 1$  the ratio  $C_{CO}/C_H$  remains constant and when it is less than one the ratio decreases.

Equation [A.2] is solved to yield the concentration profiles in the pores of the catalyst pellet. This concentration profile is then integrated over the volume of the pellet and this is used to calculate the effectiveness factor which is the ratio of the actual reaction rate (global rate) averaged over the pellet and the maximum reaction rate calculated for the surface conditions:

$$\eta_{CO} = [1/V \int_{VP} r_{CO} dV] / [R_{CO}(P_{HP_{CO}} P_{H_2O})] \quad [A.13]$$

The effectiveness factor for methane can also be obtained in a similar manner using the rate of methane production,  $r_{CH_4}$ :

$$\eta_{CH_4} = [1/V \int_{VP} r_{CH_4} dV] / [R_{CH_4}(P_{HP_{CO}} P_{H_2O})] \quad [A.14]$$

and  $r_{CH_4}$  is obtained from kinetic measurements:

$$r_{CH_4} = k_4 \exp(-(E_2 + E_1)/RT) [P_H / (1 + k_2 P_{CO} + k_3 P_H)] r_{CO} \quad [A.15]$$

Assuming an isothermal reactor for simplicity,  $\eta_{CO}$  and  $\eta_{CH_4}$  are used in a reactor mass balance to calculate the carbon monoxide conversion and methane selectivity:

$$y_{CO,i}(G_f/M_i)(dX_{CO}/dZ) = \eta_{CO} \beta_B r_{CO} \quad [A.16]$$

$$y_{CO,i}(G_f/M_i)(dX_{CH_4}/dZ) = \eta_{CH_4} \beta_B r_{CH_4} \quad [A.17]$$

where  $Y_{CO,i}$  is the carbon monoxide mole fraction in the feed,  $G_f$  is the mass velocity,  $M_i$  is the molecular weight of the feed,  $\rho_B$  is the bed density and  $X_{CO}$  and  $X_{CH_4}$  are the carbon monoxide and methane conversion, respectively.

Using a 6% Co/0.5% Re catalyst of different pellet sizes and a feed with  $H_2/CO = 2$ , the CO conversion and  $CH_4$  selectivity were measured. These conversion data were used to estimate the CO and  $H_2$  diffusivities using the following procedure:

- a. values of  $D_{e,CO}$  and  $D_{e,H}$  were assumed;
- b. effectiveness factors  $\eta_{CO}$  and  $\eta_{CH_4}$  were calculated from equations [A.9] and [A.10] and the solution of equation [A.2] given the inlet conditions of the reactor;
- c. the CO conversion and conversion to methane were calculated by integrating equations [A.16] and [A.17]; since the effectiveness factors are functions of the partial pressures of CO,  $CH_4$  and  $H_2O$  they must be recalculated along the length of the reactor taking into account of the changes in the partial pressures;
- d. methane selectivity was calculated from the ratio of conversion to methane,  $X_{CH_4}$  and carbon monoxide conversion,  $X_{CO}$ ;
- e. the calculated carbon monoxide conversion and the methane selectivity were compared with the experimental values for the various pellet sizes; and
- f. the effective diffusivities are adjusted to give the best fit of the experimental data.

An example of the agreement between the calculated and the experimental data for catalysts with a range of diameters is shown in **figure** A.1.

In one example the experiments were performed in a 3'x0.5" reactor that was packed with 1 mm diameter spherical particles uniformly loaded with 6%Co-0.5%Re. Data were obtained as the reaction temperature and the  $H_2/CO$  ratio were varied and the CO conversion and  $CH_4$  selectivity obtained as described above. When the initial

H<sub>2</sub>/CO ratio is less than 2, the ratio will decrease along the catalyst bed and, since methane selectivity depends upon this ratio, it will decrease down the bed.

Simulations of carbon monoxide conversion and methane selectivity were made for various thickness of the rim loaded metals. As shown in **figure** A.2, both conversion and methane selectivity increase with increasing rim thickness. However, the important point is that these two factors increase rapidly from a low to high value and that the rim thickness where this increase occurs is different for the two factors.

In another simulation, the carbon monoxide conversion and methane selectivity were determined for two pellet shapes: ring and cylinder. As shown in **figure** A.3, the rim thickness needed to obtain the maximum CO conversion and a low methane selectivity depends upon the pellet shape. Thus, the cylindrical shape provides a much greater difference between the rapid increase in the two factors than the ring shape does.

The inventor claims a method for making a catalyst by determining the rim thickness which optimizes both the rate of carbon monoxide hydrogenation and the reduction of methane selectivity.

Long (A.2,A.3) claims a substantially once-through hydrocarbon synthesis process which comprises reacting in a first reactor or stages, a feed comprising hydrogen and carbon monoxide, and optionally CO<sub>2</sub>, in the presence of a non-shifting hydrocarbon synthesis catalyst. The effluent is treated to recover the product from the first reactor by condensing the liquids and then reacting the remaining gases in a subsequent stage or stages in the presence of a hydrocarbon synthesis catalyst having shift activity, producing and recovering additional products.

A basis for this invention is that "The shift reaction can, however, be suppressed if the feed contains higher amounts of CO<sub>2</sub> relative to CO, and CO<sub>2</sub> is known to be added to H<sub>2</sub> + CO synthesis gas feeds for hydrocarbon synthesis. Synthesis gas feeds can contain up to 10% CO<sub>2</sub>, that is, about 0.1-10% CO<sub>2</sub>." The feed to the first stage(s) has H<sub>2</sub>/CO in a 1.5:1 to 1.5:1 mole ratio, preferably 1.9: to 2.3:1, and CO<sub>2</sub> in the range 1.0-10 mole%, preferably 5-10 mole%. This mixture is subjected to synthesis with a non-shifting catalyst, preferably cobalt on alumina, silica or titania (preferred), and preferably promoted by metals as Ru, Rh, Ce or Hf, most particularly Rh (A.4). Conversion of CO in the first stage(s) are preferably at least 90%. Following conversion by the non-shifting catalyst, the liquid products, containing C<sub>5</sub>+ hydrocarbons, water, oxygenated compounds and small amounts of dissolved gases.

The feed for the stage 2 reactor(s) with shift catalyst is illustrated in **Table A.1**. Based on our calculations, the mole fraction of water in the feed is 0.0024 (1.83 mm if operating at 20 atm). For a water-vapor saturated stream, we estimate the temperature of the separation to be -10 to -15°C, a surprisingly low temperature. The gas shown in **Table A.1** is fed to a stage 2 reactor(s) where subsequent hydrocarbon synthesis produces a product with an olefin:paraffin ratio of 1.5:1 to 4:1, the lower ratios being favored for higher hydrocarbons and the higher ratios favored for the lower carbon number hydrocarbons. The H<sub>2</sub>/CO ratio entering the stage 2 reactor(s) will be essentially the same as the stage 1 reactor(s) because of the non-shifting character in the stage 1 operations. However, because of the conversion in stage 1 reactor(s), less gas will enter stage 2 reactor(s) with the result that the relative concentration of CO<sub>2</sub> will be higher in stage 2 than in stage 1 reactors. Sufficient hydrogen must be present in the feed to stage 2 reactor(s) to react with both CO and CO<sub>2</sub>. Reaction conditions in

stage 2 reactor(s) will be similar to those in stage 1 reactor(s); e.g., 10-35 bar, 220-340°, SHSV 200-2000 dry feed (water less than 5 vol% of feed).

### Slurry Reactor

Herbolzheimer et al. (A.5) claim the use of a second solid in a slurry phase hydrocarbon synthesis process. A gas is injected at or near the bottom of the bubble column containing a slurry liquid, a catalytically active first solid and at least a second solid. The energy to maintain the dispersion of the solids is supplied by the gas in the absence of liquid recycle. The second solid is added in sufficient quantity to increase the bed height by at least 10%.

The authors state that slurry phase reaction, particularly those occurring in bubble columns, are well-known and do not need to be discussed. In column 6, line 23, the authors state that, "Slurry reactors are well known..." This is surprising since it would appear to imply that at the time of filing this patent [February 25, 1991] the use of slurry reactions are well known and, since bubble column reactors are also well known, only specific improvements to the operation of slurry bubble column reactors should be patentable inventions. Catalyst settling is a problem that can be encountered in bubble column reactors. Particles tend to settle to the bottom because of the influence of gravity. Opposing the settling tendency is the dispersion forces created by the rising bubbles of gas injected at or near the bottom of the reactor. The balancing effect of these two forces results in an exponential distribution of catalyst solids concentration.

The authors utilize the data employing a dispersion coefficient and the settling velocity.  $D$ , the dispersion coefficient, depends on the superficial gas velocity through the system and on the effective diameter of the reactor column. The authors do not



define this term in more detail, and presumably are considering the dispersion coefficient for the solids. The settling velocity of the catalyst particles,  $U_s$ , is given as

$$U_s = U_o(1 - c)^n \quad [A.18]$$

where

$$U_o = dp^2(\rho_s - \rho)/18F \quad [\rho_s \text{ is given as } \rho_s \text{ in the patent}] \quad [A.19]$$

where  $c$  is the volume fraction of solids in the slurry,  $d_p$  is the particle diameter,  $\rho_s$  is the density of the solids,  $g$  is the gravitational constant,  $F$  is the viscosity of the suspending liquid, and  $n$  is a constant ranging from 4 to 8.

In the description, they indicate that most reactors operate in a regime somewhere between plug-flow and fully-backmixed (or CSTR) conditions. A plug-flow condition can be attained by using fixed-bed catalyst or a very large  $L/d$  (where  $L$  and  $d$  are the length and effective diameter of the reactor, respectively). In the plug-flow reactor the concentration (or partial pressure) of hydrogen and carbon monoxide, the reactants for Fischer-Tropsch Synthesis, decrease along the path of reactor flow due to reaction, and this decreases the driving force of the reaction. On the contrary, complete backmixing results in the same concentration of reactants along the entire length of the reactor resulting in a constant driving force and reflects the relatively low driving force at exit conditions.

Productivity is generally favored in plug-flow systems and selectivity is favored in backmixed systems. Later Exxon patents pertain to the operating conditions for plug-flow bubble column slurry reactors .

In the preferred mode for this patent, there is an absence of liquid throughput; thus, in the preferred mode, all of the energy from maintaining solids as a dispersion in the liquid is provided by the injection of gas at or near the bottom of the slurry reactor.

The catalysts utilized in the examples are typical of those described in many Exxon, and other, patents. The preferred catalyst is cobalt supported on titania and promoted with rhenium. The preferred catalyst particle size is in the range of 20 to 100 microns.

The data described in the examples were obtained in a 5 meter tall, non-reactive bubble column with 15 cm internal diameter (i.e., the L/d ratio was greater than 20, corresponding to nearly plug-flow conditions). Nitrogen gas was injected vertically into the column through a half inch hole at the bottom of a conical insert. This cone was used to insure fluidization of all the particles charged to the system. Pressure and temperature were monitored at 1 meter intervals along the column length, and slurry samples were withdrawn at these locations. The slurry liquid was C<sub>20</sub>-C<sub>40</sub> paraffinic wax produced by Fischer-Tropsch synthesis using a cobalt catalyst. The solid was either TiO<sub>2</sub> or glass beads. No liquid was added during the measurements.

The solids distribution of 80 micron glass beads in FT product was determined at a temperature of 400°F (204°C) and 280 psig (for gas velocities below 8 cm/sec) or 150 psig (for gas velocities above 8 cm/sec). The decay length of the particle concentration profile was obtained by taking the slope of a line segment joining the data points when plotted as the logarithm of the solids concentration versus height. In **figure** A.4, the decay length in each zone is plotted versus the average concentration in the zone for superficial gas velocities of 2-16 cm/sec.

They correlated the data by

$$D/U_s(\text{feet}) = 0.2(1 + 20c^2 + 3000c^4)/U_o(\text{cm/sec}) \quad [\text{A.20}]$$

for  $U_g < 4$  cm/sec and

$$D/U_s(\text{feet}) = 1.2(1 + 3c^2 + 500c^4)/U_o(\text{cm/sec}) \quad [\text{A.21}]$$

for  $U_g < 4$  cm/sec.

$U_o$  is Stokes settling velocity and  $c$  is the volume fraction of solids in the slurry.

The results of the above experiment with glass beads was then used in models to predict solids distribution for several examples of various solids combinations. For catalyst and inert solids of the same density ( $2.7 \text{ g/cm}^3$ ) and diameter (50 microns) that are (1) dispersed in a solvent with a liquid viscosity of 0.9 cp and density of  $0.7 \text{ g/cm}_3$ , (2) with an average catalyst loading of 0.05 by volume (gas-free basis), (3) an expand bed height of 30 feet, (4) a gas inlet velocity of 8 cm/sec, and (5) an overall conversion of 0.8, they obtained catalyst distributions with 0, 0.05, 0.1, 0.2 and 0.3 volume fraction of inert solids added.

The data in **figure** 5.A show that with only catalyst the effective bed height is about 13 feet, and with the catalyst more heavily concentrated at the bottom of the reactor. The addition of even a small amount of inerts increase the bed height. As the inert solids content is increased the bed expands further in height and the catalyst concentration profile becomes flatter.

In another example, they use the same catalyst and inert solid except the inerts are 1 micron in size. This example would be approximated by the use of 80 micron iron catalyst spheres made up of 1 micron particles that, because of attrition, produce individual 1 micron fines. Effects similar to those of equal sized particles are obtained. A similar calculation was made using an active catalyst of density  $2.7 \text{ g/cm}^3$  and lower activity catalyst with a density of  $1.0 \text{ g/cm}^3$ . They also made calculations for the case when the original activity is decreased by factors of 2, 4, and 6. The use of the less active component also causes the bed to expand.

In the examples provided, the authors do not provide an identification of the meaning of the curves for volume fraction of catalyst vs. height in figures A.2-A.5 of the patent or in the figure legend. Thus, the reader must assume the identity of the curves.

It appears that this patent is the basis for the several patents that pertain to inert solids. For example, a structurally modified alumina prepared by incorporating a Group IIA metal or metals, particularly Mg or Ba, is claimed to have increased resistance to sintering and agglomeration (A.6). These materials are considered as aiding catalyst fluidization, as a catalyst support, and as heat transfer agents in syngas production or utilization in the slurry phase (A.7-A.12).

Stark (A.13,A.14) was issued a patent to cover the use of pentane (or similar light hydrocarbon) to remove the exothermic heat of reaction of the Fischer-Tropsch process and to expand the pentane to recover the energy to drive air plant compressors. Steam/water is the usual material for heat removal, and is utilized in the commercial reactors at Sasol. However, Stark indicates that it is desirable to have a coolant that has a boiling point and vaporizes at a pressure higher than the reaction pressure; this will ensure that no problem will arise if a leak allows coolant to enter the reaction zone. In order for vaporization to occur with pentane, it is necessary that the coolant side be below the critical conditions (197°C; 44.1 atm. (679 psi)).

Stark (A.13,A.14) claims a method for removing heat from a hydrocarbon synthesis process reaction zone. A cooling medium is passed through the reactor zone in an indirect heat exchange, thereby vaporizing the cooling medium. The cooling medium is chosen so that it possesses the properties of inertness, condensable and vaporizes at a pressure which is at least as great as the pressure in the reaction zone.

Water/steam is frequently employed as the heat transfer medium. However, the authors claim that there is a reasonable expectation of leaks in a F.T. reactor because of the presence of numerous tubes and welds. In the case of water/steam, the reactor pressure is higher than the water/steam side so that F.T. products will leak into the cooling section whenever a leak occurs. The accumulation of products in the cooling side will eventually require the unit to be shut down for cleaning and/or repairs. In this instance, the cooling medium is chosen to have a higher vapor pressure than inside the reactor so that any leakage will be from cooling side to reactor. An appropriate cooling medium is n-pentane, a product of the F.T. synthesis.

The high pressure energy is recovered from the cooling medium through an expander. Preferably a substantial portion of the energy recovered from the expander is used to drive compressors for an air plant which separates oxygen from nitrogen.

The U.S. patent, but not the European patent application, indicates that the F.T. synthesis is carried out in a slurry phase system.

#### Hydrocracking and Hydroisomerization

Davis et al. (A.15) claim a hydroisomerization process for the conversion of a  $C_{5+}$  paraffinic feedstock to middle distillates. This involves contacting and reacting the feedstock and hydrogen at hydroisomerization reaction conditions with a catalyst comprising a Group IB, VIB or Group VIII metal component, or two or more metals, supported on an acidic particulate solid with an average particle diameter of the size range 30 to 150 Fm which is dispersed in a paraffinic liquid hydrocarbon.

Davis et al. (A.15) report that in normal hydrocracking with large catalyst particles, secondary reactions, arising from diffusional limitations, produce large amounts of gas and naphtha, and decrease the yield of the desirable middle distillate

fractions. To overcome this limitation, staged fixed-bed reactors are operated at relatively low space velocities. They cite an earlier process [U.S. Patent 5,378,348] utilizing a separation into two boiling range fractions (500°F<sup>-</sup> and 500°F<sup>+</sup>) and separately hydroisomerizing to make middle distillates.

The hydroisomerization of the present invention is conducted in a slurry phase, preferably with greater than 25% catalyst slurry of particles in the micron size range (preferably 40-60 micron). The catalyst is bifunctional, possessing metallic hydrogenation and acidic functions. The metal oxide support, preferably a silica-alumina material, is prepared as described in reference -[U.S. Patent 3,843,509].

It is reported that one slurry reactor can be used to obtain approximately as much conversion as in three packed bed reactors in series under similar reaction conditions. An additional advantage of the slurry reactor is that a water-steam cooling coil can be used to remove the exothermic heat of reaction and to control the temperature. Using a packed fixed-bed reactor, a complex system of traps and quenching techniques are required to control the heat that is released during the reaction.

Data for the conversion of n-hexane show that the conversion decreases with increasing hydrogen pressure. At a given temperature, the fraction of single methyl branches decreases with increasing feedstock conversion; significant amounts of multi-methyl branched compounds appear at higher feedstock conversion. In contrast, in a fixed bed reactor undesirable cracked products result at higher conversion levels. Even with the slurry technology, the fraction of cracking increases with feedstock conversion at levels above about 80%.

The kinetics of the Fischer-Tropsch wax cracking with a Pd/silica-alumina catalyst was obtained to design a reactor for a commercial scale process. They report that conversion followed zero order kinetics with an apparent activation energy of 30-35 kcal/mole for the conversion range of 30-70%.

Davis and Ryan (A.16) claim a process for producing middle distillate transportation fuels from a waxy product of a hydrocarbon synthesis process. The process consists of:

1. separating the product into a heavier (500°F<sup>+</sup>) and at least one lower (500°F<sup>-</sup>),
2. catalytically isomerize the heavier products in the presence of hydrogen,
3. catalytic hydrotreat the lighter fraction to remove heteroatoms (primarily O), and,
4. catalytically isomerize the product from step (3) to a product with a freeze point of -30°F or lower.

The authors indicate that a cobalt catalyst tends to produce heavier products, e.g., containing C<sub>20+</sub>, whereas ruthenium tends to produce more distillate type products, e.g., C<sub>5</sub>-C<sub>20</sub>. A typical product slate for a cobalt catalyst is given as (the values may vary by ±10% for each fraction) is given in **Table A.2**.

Surprisingly, they found that hydrotreatment of the heavier fraction (containing about 0.45 wt% oxygen) prevents the production of a product with the excellent cold flow properties that was formed by hydroisomerization of the untreated material. They indicate the need to limit the conversion for the 700°F<sup>+</sup> to the 700°F<sup>-</sup> products to the 35-80% range as a measure to limit cracking to produce gases and thereby a lower yield of distillates.

The lighter fraction can be the 320-500°F or, preferably, the entire liquid fraction boiling below 500°F. Following a conventional hydrotreatment, the naphtha is flashed

off and the remaining material is hydroisomerized using a catalyst appropriate for light fractions, such as the ones described in reference A.17.

The most active catalysts were those materials containing a surface silica additive. However, it is stated that selectivity is more important than activity. Activity was improved when a 4% surface  $\text{SiO}_2/\text{CoNiMo}/10\%\text{SiO}_2\text{-Al}_2\text{O}_3$  catalyst was used at 700 psig rather than 1,000 psig. Increasing the LHSV to 3.0 and increasing the temperature to provide activity similar to that of LHSV = 0.5 to 1.0 dramatically effected the products; the yield of jet fuel was decreased in favor of gas and naphtha production and the jet fuel had an increased freeze point. The cause for this was not understood but it was speculated that diffusional problems were the major factor.

An international patent application (A.18) claims the production of a high purity solvent composition which comprises a mixture of paraffins of carbon number ranging from about  $\text{C}_8$  to  $\text{C}_{20}$ . The solvent has a molar ratio of iso-/n-paraffins ranging from about 0.5:1 to 9:1 and the isoparaffins of the mixture contain greater than 50% of the mono-methyl species. This patent application employees catalysts and processing schemes that are included in reference (A.19).

The Fischer-Tropsch product was obtained from the conversion of a synthesis gas ( $\text{H}_2:\text{CO} = 2.11\text{-}2.16$ ) with a titania supported cobalt-rhenium catalyst. The reaction conditions were in the range of 422-428°F, 287-289 psig and feed linear velocity of 12 to 17.5. The alpha of the Fischer-Tropsch synthesis was 0.92.

The 700°F+ boiling fraction was hydroconverted over a Pd-silica-alumina catalyst (0.5 wt.% Pd, 38 wt.%  $\text{Al}_2\text{O}_3$ ) to produce 39.4 wt.% conversion of the 700°F+ to 700°F- materials (Table A.3).



Wittenbrink et al. (A.20) describe a processing scheme whereby some oxygenates (primary alcohols) remain in the finished fuel. These oxygenates function to improve the lubricity of the diesel fuel.

The process scheme illustrated in their **figure** A.6 leads to some confusion. Shown leaving the Fischer-Tropsch reactor (vessel 2) are two streams: 3 (700°F+; 370°C) and 4 (700°F-). It is reported that the reactor is operated in the range 422-428°F (217-220°C) and 287-289 psig using a titania supported cobalt/rhenium catalyst (A22). The syngas had a composition of  $H_2/CO = 2.11-2.16$ . The alpha for FTS was 0.92. The FTS products were separated into three fractions having approximate boiling ranges: (1)  $C_5-500^\circ F$  (designated F-T cold separator liquids); (2)  $500-700^\circ F$  (F.T. hot separator liquids) and  $700^\circ F+$  (F.T. reactor wax). It appears that streams 3 and 4 in **figure** A.6 must be sent to a fractionator (not shown in the figure) to generate three streams.

The hydroisomerization and recombining of fractions are the same, or essentially the same, as described by Davis et al. (A.15) above.

## References

- A.1. Herskowitz, M., Method for hydrocarbon synthesis reactions; US patent 5,652,193, July 29, 1997.
- A.2. D. C. Long, U. S. Patent 5,498,638, March 13, 1996.
- A.3. D. C. Long, European Patent Office Publication No. 0 679 620 A2, April 26, 1995.
- A.4. See, for example, U.S. 4,637,993; U.S. 4,717,702; U.S. 4,477,595; U.S. U.S. 4,663,305; U.S. 4,822,824; U.S. 5,036,032; U.S. 5,140,050; U.S. 5,292,705.

- A.5. E. Herbolzheimer, F. J. Kaiser, Jr., and E. Iglesia; U. S. Patent 5,157,054, October 20, 1992.
- A.6. Clavenna, L. R., S. M. Davis, R. A. Fiato and G. R. Say; Structurally modified alumina supports, and heat transfer solids for high temperature fluidized bed reactions; U.S. 5,395,406, March 7, 1995.
- A.7. Clavenna, L. R., S. M. Davis, G. R. Say and R. A. Fiato; Synthesis gas from particulate catalysts, and admixtures of particulate catalysts and heat transfer solids; U.S. 5,348,717, Sept. 20, 1994.
- A.8. Davis, S. M., L. R. Clavenna, G. R. Say and R. A. Fiato; High surface purity heat transfer solids for high temperature fluidized bed reactions; U.S. 5,360,778, Nov. 1, 1994.
- A.9. Davis, S. M., L. R. Clavenna, G. R. Say and R. A. Fiato; High surface purity heat transfer solids for high temperature fluidized bed reactions; U. S. Patent 5,496,531, March 5, 1996.
- A.10. Clavenna, L. R., S. M. Davis, R. A. Fiato and G. R. Say; Particulate solids for catalyst supports and heat transfer materials; U. S. Patent 5,395,813, March 7, 1995.
- A.11. Davis, S. M., L. R. Clavenna, R. A. Fiato and G. R. Say; High performance alumina heat transfer solids for high temperature fluidized bed synthesis gas reactions; U.S. 5,360,777, Nov. 1, 1994.
- A.12. Clavenna, L. R., R. A. Fiato and G. R. Say; Particulate solids for catalyst supports and heat transfer materials, U.S. patent 5,476,877, Dec. 19, 1995.
- A.13. T. M. Stark, U.S. Patent 5,409,960, April 25, 1995.
- A.14. T. M. Stark, European patent application Number 94301541.2.

- A.15. S. M. Davis, J. W. Johnson, C J. Mart, D. F. Ryan and R. J. Wittenbrink;  
European Patent Application EP 0 753 563 A1, filed April 7, 1996.
- A.16. S. M. Davis and D. F. Ryan, U.S. Patent 5,378,348, January 3, 1995.
- A.17. U.S. Patent 5,187,138]
- A.18. WO 97/21787
- A.19. U.S. Patent 5,378,348
- A.20. R. J. Wittenbrink, R. F. Bauman, P. J. Berlowitz and B. R. Cook, International  
Publication No. WO 97/14769, April 24, 1997.
- A.21. U.S. Patent 4,568,663.

Table A.1			
Reactor Simulation Results			
		Stage 2 Product	
	Stage 2 Feed	Shifting Catalyst	Non-shifting
Component Rates, Moles/Hr			
H <sub>2</sub>	11584	3021	6781
CO	2823	564	524
CO <sub>2</sub>	16324	15065	16326
H <sub>2</sub> O	113	4887	2400
Hydrocarbon + Alcohol	13701	14045	13924
Inert	2434	2434	2434
Moles Converted			
CO		2259	2299
CO <sub>2</sub>		1259	-2
Total		3518	2297
% (CO+CO <sub>2</sub> ) Converted		18.4	12.0
Hydrocarbon + alcohol		344	223
Yield, Moles/Hr			

Table A.2

Typical Product Slate from FT Process Liquids Produced with a Cobalt Catalyst  
(from ref. A.17)

Fraction	Wt.%
IBP-320°F	13
320-500°F	23
500-700°F	19
700-1050°F	34
1050°F+	11
TOTAL	100

Table A.3	
Fischer-Tropsch Synthesis conditions	
Operating Conditions	
Temperature, °F	638
LHSV, v/v/h	1.2
Psig	711
H <sub>2</sub> treat rate, SCF/B	2,100
Yields, Wt.%	
C <sub>1</sub> -C <sub>4</sub>	0.97
C <sub>5</sub> -320°F	10.27
320-500°F	14.91
500-700°F	29.99
700°F+	43.86
TOTAL	100
700°F Conversion, Wt.%	39.4
15/5 Distillation Yields, Wt.%	
IBP-650°F	50.76
650°F+	49.24

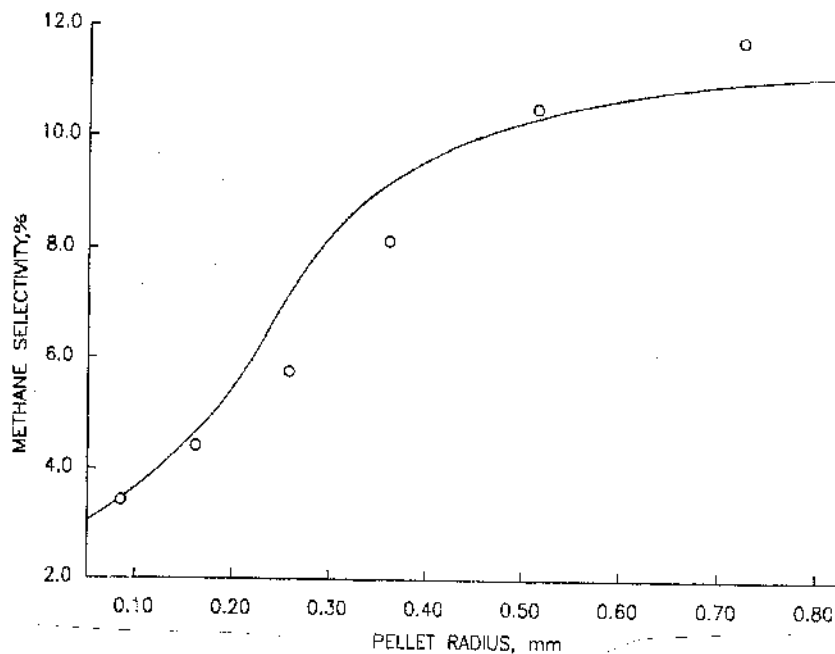


Figure A.1. Model predictions for methane selectivity as a function of pellet radius compared to experimental data (6% CO-0.5% Re catalyst;  $T = 200^{\circ}\text{C}$ ;  $(P_{H_2}/P_{CO})_{feed} = 2.0$ ;  $P_t = 19 \text{ atm}$ ) (from ref. A.????).

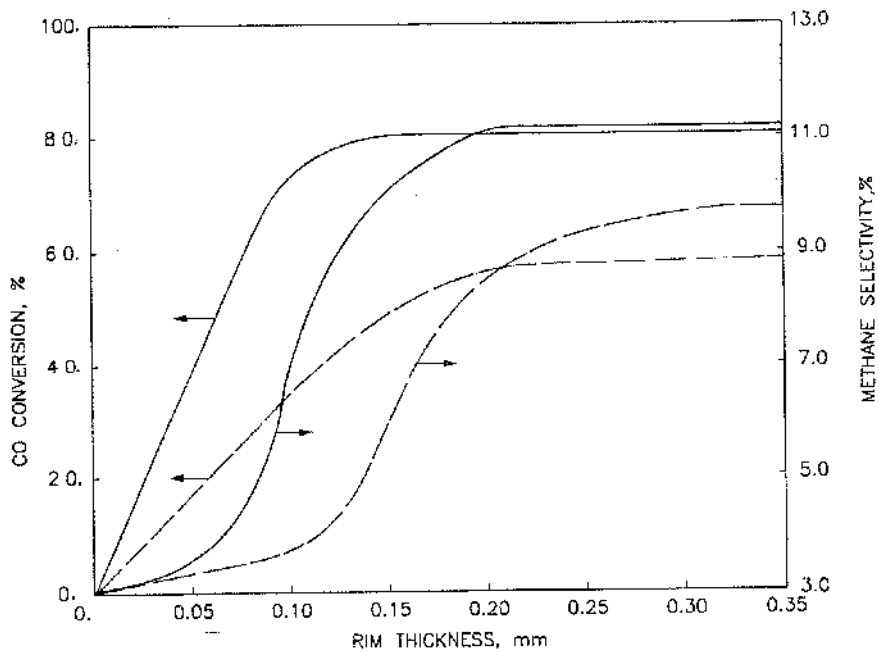


Figure A.2. CO conversion and methane selectivity as a function of rim thickness for spherical particles ( $d_p = 1.0 \text{ mm}$ ;  $T = 200^{\circ}\text{C}$ ;  $\text{GHSV} = 770 \text{ v/v/hr}$ ; ---  $A = .6 \times 10^{+5} \text{ mole/s/s}\cdot\text{g}\cdot\text{atm}^2$ ; )  $A = 1.2 \times 10^{+5} \text{ mole/mole/s/s}\cdot\text{g}\cdot\text{atm}^2$ ) (from ref. A.1).

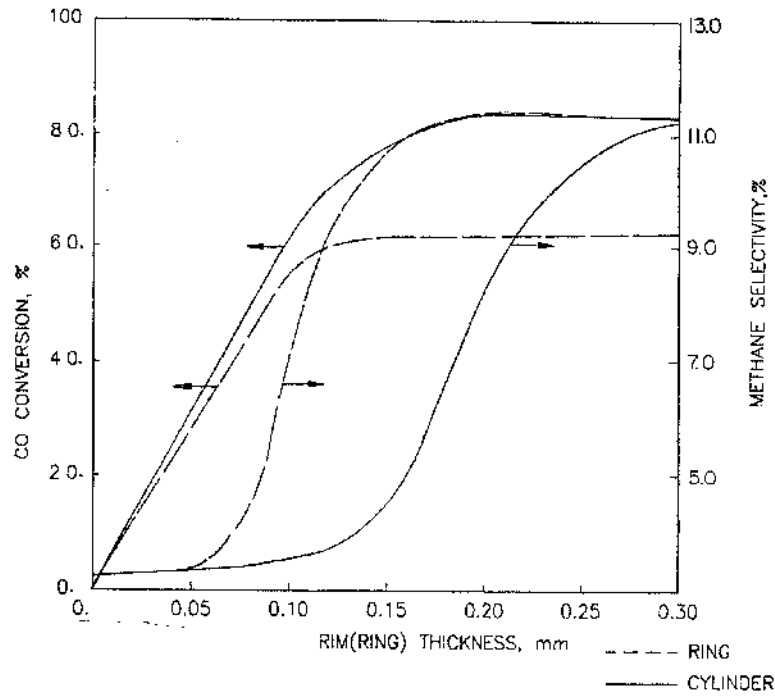


Figure A.3. CO conversion and methane selectivity as a function of rim thickness for ring (---) and cylinder (—) pellets ( $d_p = 1.0$  mm;  $T = 200^\circ\text{C}$ ;  $\text{GHSV} = 770$ ;  $A = 1.2 \times 10^5$  mole/s $\cdot$ g $\cdot$ atm $^2$  (from ref. A.1).

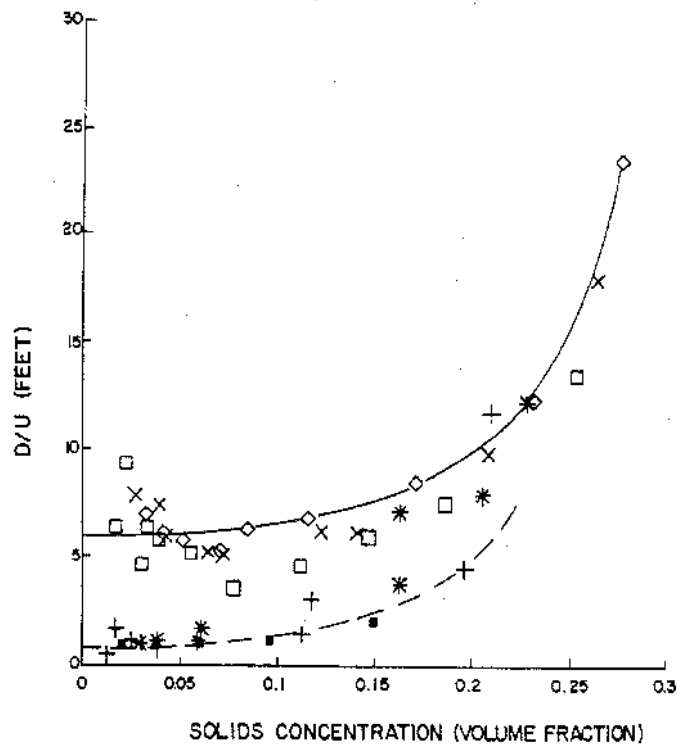


Figure A.4. Plot of decay length versus volume fraction solids concentration (#, 2 cm/sec; G, 8 cm/sec; +, 4 cm/sec; X, 12 cm/sec; \*, 6 cm/sec; ", 16-18 cm/sec).



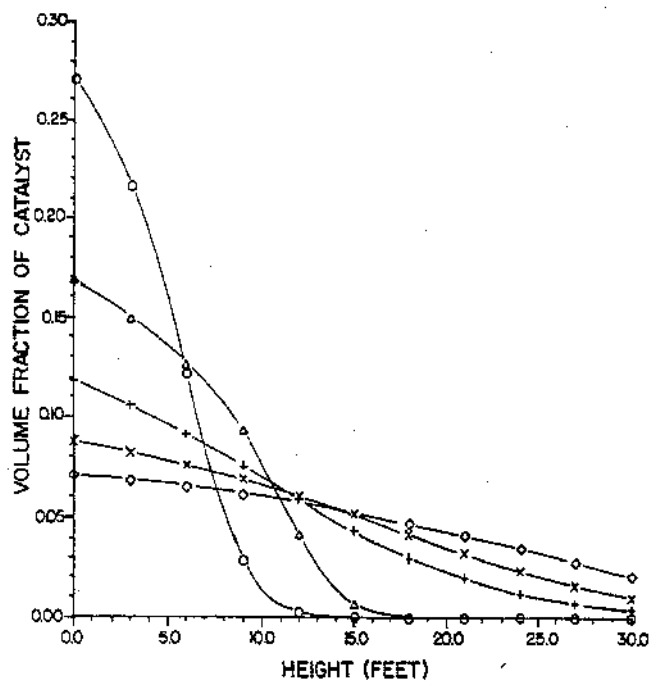


Figure A.5. A plot of volume fraction versus bed height when a second inert solid to a first catalytically active solid in a bubble column, the inerts being of the same density and diameter as the catalytic solid.

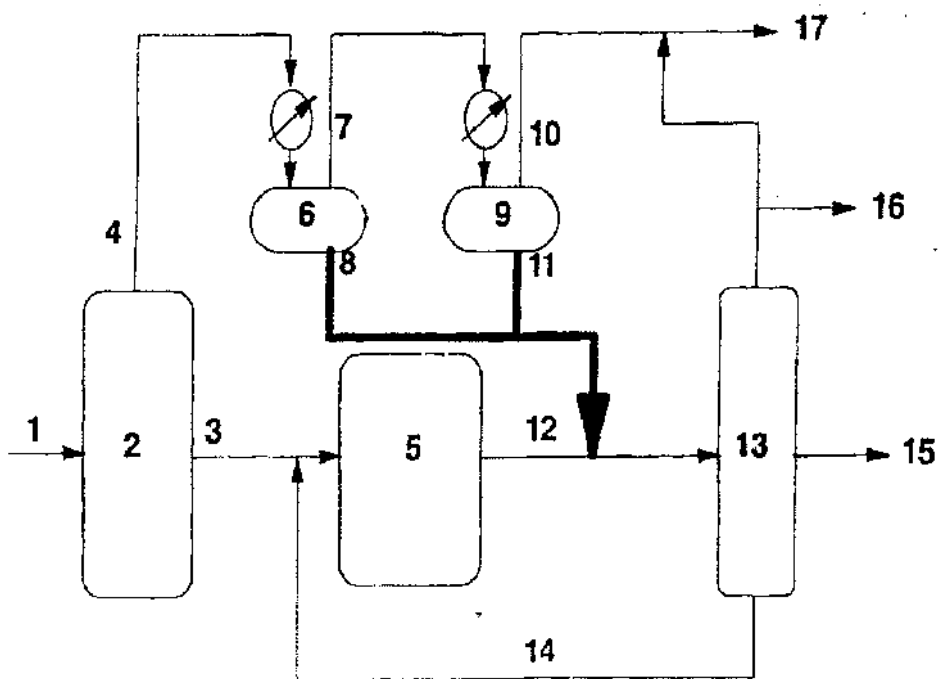


Figure A.6. Schematic of the process (from ref. A.21).